

# Ultrasonicated double wall carbon nanotubes for enhanced electric double layer capacitance

Srikrishna Pandey,<sup>1,a)</sup> Uday N. Maiti,<sup>1</sup> Kowsalya Palanisamy,<sup>2</sup> Pavel Nikolaev,<sup>2,b)</sup> and Sivaram Arepalli<sup>3,a)</sup>

<sup>1</sup>Center for Nanomaterials and Chemical Reactions, Institute for Basic Science (IBS) and Department of Materials Science & Engineering, Korea Advanced Institute of Science & Technology, 373-1 Guseong-dong, Yuseong-gu, Daejeon, South Korea

<sup>2</sup>Department of Energy Science, Sungkyunkwan University, Suwon 440746, South Korea

<sup>3</sup>National Institute of Aerospace, 100 Exploration Way, Hampton, Virginia 23666, USA

(Received 17 April 2014; accepted 28 May 2014; published online 10 June 2014)

An intense ultrasonication of the double wall carbon nanotubes (DWCNTs) causes fractures and splitting of the individual tubes. This not only generates open tips and edges in DWCNTs but also incorporates defects in the tube walls. The electric double layer capacitor (EDLC) electrodes of intensively ultrasonicated DWCNTs (U-DWCNTs) form organized layered-porous structures. The EDLC behavior of U-DWCNTs electrodes shows dramatic improvements (specific capacitance 10 times and 222 times larger than the pristine DWCNTs at scan rates  $5 \text{ mV s}^{-1}$  and  $500 \text{ mV s}^{-1}$ , respectively) due to the increased wettability of electrodes and accessibility of the electrolyte ions.

© 2014 AIP Publishing LLC. [<http://dx.doi.org/10.1063/1.4882278>]

Charge storage in electric double layer capacitance-based supercapacitors (EDLC) is based on charge separation in a Helmholtz double layer at the interface between the conductive electrode surface and the electrolyte. This kind of charge accumulation at the interface is similar to the classical electrostatic capacitors, albeit the charge separation is smaller, on the order of a few angstroms. In recent years, EDLC-based supercapacitors have become an area of intensive research due to their high specific capacitance, high power density, and long life cycle.<sup>1–3</sup> EDLCs have been sought for various power applications such as in memory backup devices, electric vehicles, aerospace equipment, emergency power supplies, and hybrid energy storage devices which can eliminate the gap between traditional dielectric capacitors and batteries.<sup>1–8</sup>

Carbon nanotubes (CNTs) are being considered as the choice of high-power electrode material for next generation EDLCs due to their special architecture, high electrical conductivity, and readily accessible high surface area.<sup>1–3,9,10</sup> However, ion accessibility to the surface of pristine CNT-based electrodes is hindered due to bundle formation by inter-tube Van der Waals forces and capping of tube ends. To alleviate this problem, chemical modifications are frequently employed, but their effectiveness is limited by severe loss of the properties of pristine CNTs due to attachment of various chemically active functional groups.<sup>1,9</sup> Another approach could be incorporation of defects by physical methods to increase electrolyte ions accessible area of CNTs.<sup>1,9,11,12</sup> In this Letter, we demonstrate an alternative approach to provide electrolyte ions access to the interior of CNTs' surfaces by mechanical splitting of CNTs using

intense ultrasonication process. Intense ultrasonication produces defects and structural changes, resulting in improved wettability of the electrodes. Interestingly, the incorporation of structural changes during the ultrasonication process facilitated a layered porous structure when electrodes of supercapacitor were prepared. These factors contributed remarkably to enhance the formation of EDLC at the electrode-electrolyte interface. Owing to the improved accessibility of ions, the specific capacitance of the intensively ultrasonicated double wall carbon nanotubes (U-DWCNTs) electrodes was found to be up to 222 times higher compared to the pristine DWCNTs at high scan rates ( $500 \text{ mV s}^{-1}$ ).

The DWCNTs were procured from the MER Corporation, Tucson, AZ, USA. The average length of individual pristine DWCNT is  $\sim 100 \mu\text{m}$ . The average inner diameter (ID) of the DWCNTs is  $1.6 \pm 0.1 \text{ nm}$ ; and outer diameter is (OD)  $2.2 \pm 0.1 \text{ nm}$ . Samples contain no more than 10% single wall CNTs, and multi-wall CNTs are absent. To perform an intense ultrasonication process, 10 mg of DWCNTs were dispersed in 20 ml of dimethylacetamide (DMA) solvent for an hour using a high shear homogenizer (IKA T25 digital Ultra-Taurrx) at 20 000 rpm. Afterward, the dispersed DWCNTs were ultrasonicated using a probe sonicator for 2 h with 2 000 000 joules energy. To avoid sample heating, the sonication process was performed in an ice bath.

The effect of the intense ultrasonication on DWCNTs was initially investigated using field-emission scanning electron microscopy (FE-SEM, JEOL:JSM 7000F). Figs. 1(a) and 1(b) show SEM images of the pristine DWCNTs as received from MER Corporation. Figs. 1(c) and 1(d) show SEM images of DWCNTs after intense ultrasonication. It is evident from the images that ultrasonication of  $\sim 100 \mu\text{m}$  long pristine DWCNT bundles splits them down to a few micron length, which results in opening tube tips. SEM images of the electrodes prepared out of U-DWCNTs and used in electrochemical measurements show a very uniform porous and layered structure (Figs. 1(e) and 1(f)). Deep pores

<sup>a)</sup>Electronic addresses: srikrishnapandey@gmail.com and sivaram.arepalli@gmail.com

<sup>b)</sup>Present address: Air Force Research Laboratory, Materials and Manufacturing Directorate, Wright Patterson AFB and UES, Inc., Ohio 45433, USA.

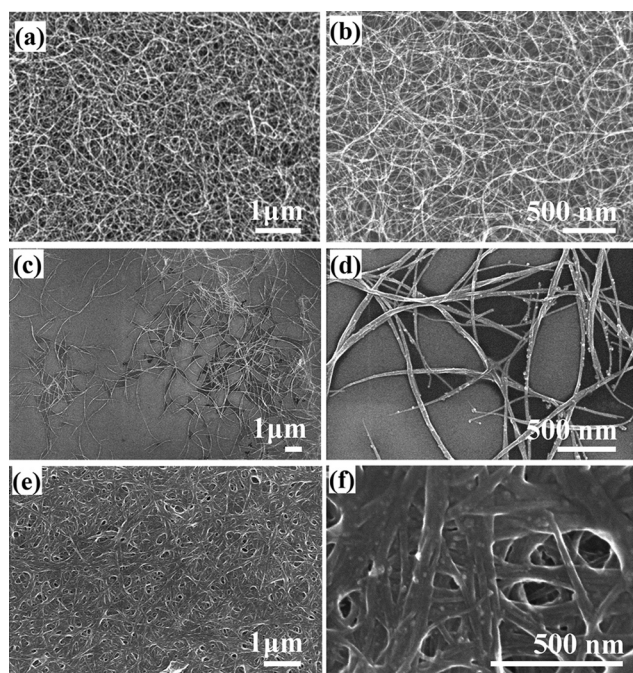


FIG. 1. SEM images. (a) and (b): Pristine DWCNTs film. (c) and (d): DWCNTs after intense ultrasonication. (e) and (f): Electrode formed out of ultrasonicated DWCNTs.

of several layers can clearly be observed in Fig. 1(f), and some of the pores seem to be interconnected. Average pore dimensions are in the range of few hundred nanometers.

In order to identify the structural changes during the process, the U-DWCNTs were further characterized by field-emission high resolution transmission electron microscopy (FE-HRTEM, JEOL:JEM2100F operated at 200 kV) and Raman spectroscopy (Renishaw RM1000 with 633 nm excitation wavelength). Fig. 2(a) shows HRTEM images of dispersed U-DWCNTs bundles. If we compare HRTEM images of U-DWCNTs with pristine DWCNTs bundle obtained by low power sonication (Fig. 2(a), inset), it seems that besides splitting into several segments, intensive ultrasonication also damage the walls of U-DWCNTs. The nano-sized particles seen in images are iron catalyst used for the synthesis of DWCNTs mat. Since these particles do not have any negative contribution to the capacitance, they were not separated from the samples. The level and type of the defects introduced by intense ultrasonication were identified using Raman spectroscopy. Fig. 2(b) shows the Raman spectra of pristine and U-DWCNTs samples. The  $I_D/I_G$  ratio of the ultrasonicated sample was increased by a factor of 10, revealing that intense ultrasonication results in large scale defects and damage to the CNT walls. However, no shift in D-band position was observed. Absence of the shift in D band position is possible only if the origin and nature of the introduced defects is similar to that in the pristine sample.<sup>13</sup> Therefore, the additional defects acquired during ultrasonication seems to be physical in nature. After characterizing the sample, we can conclude that the U-DWCNTs electrodes have a layered porous structure with opened-tip DWCNTs and appreciable level of additional edges and defects compared to the pristine sample.

After fully characterizing the sample, the electrochemical measurements were performed using electrochemical

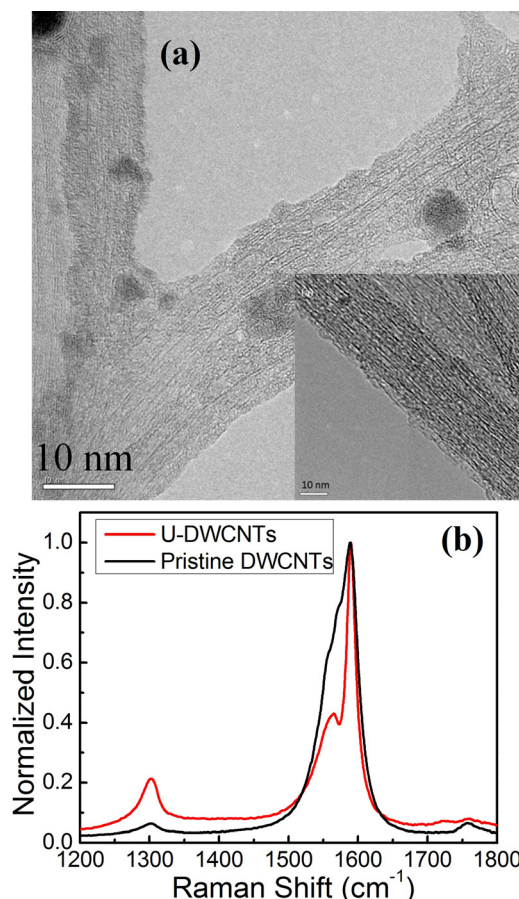


FIG. 2. (a) HRTEM image of U-DWCNTs (pristine DWCNTs are shown on inset). (b) Raman spectra of pristine and U-DWCNTs.

setup (Bio-Logic Science Instruments, VMP3) on both the pristine and ultrasonicated DWCNTs. All cyclic voltammetry (CV) measurements were carried out in 1 M  $H_2SO_4$  electrolyte using three-electrode system; where sample was transferred onto the glassy carbon electrode, with Pt as a counter electrode and Ag/AgCl as a reference electrode. No binder was used in the electrode deposition. Mass of the electrodes was determined using a microbalance (1  $\mu g$  accuracy) by measuring weight difference of the glassy carbon electrodes before and after the DWCNTs deposition. Based on the error involved in measuring mass of the electrodes, the error in specific capacitance calculations could be  $\pm 5\%$ . Fig. 3(a) shows the CV curves and Fig. 3(b) shows the corresponding calculated specific capacitance of the pristine DWCNTs mat electrodes as a function of voltage at scan rates of 50, 100, 200, 300, and 500  $mV s^{-1}$ . The calculated average specific capacitances obtained by integration over a complete cycle were 27, 18, 10, 3.8, 2, and 0.8  $Fg^{-1}$ , respectively. The strong deviation from the ideal rectangular shape of CV curves even at very low scan rates reflects poor ion propagation and presence of high electrode-electrolyte resistance. Alternatively, the contact resistance could also play a role in determining the shape of the CV curves, because larger resistance leads to a narrower loop with an oblique angle. This contribution, however, should be very small because glassy carbon was used as current collector. Moreover, as we increase the scan rate, the deviation and oblique angle increase rapidly. This is an indication of high

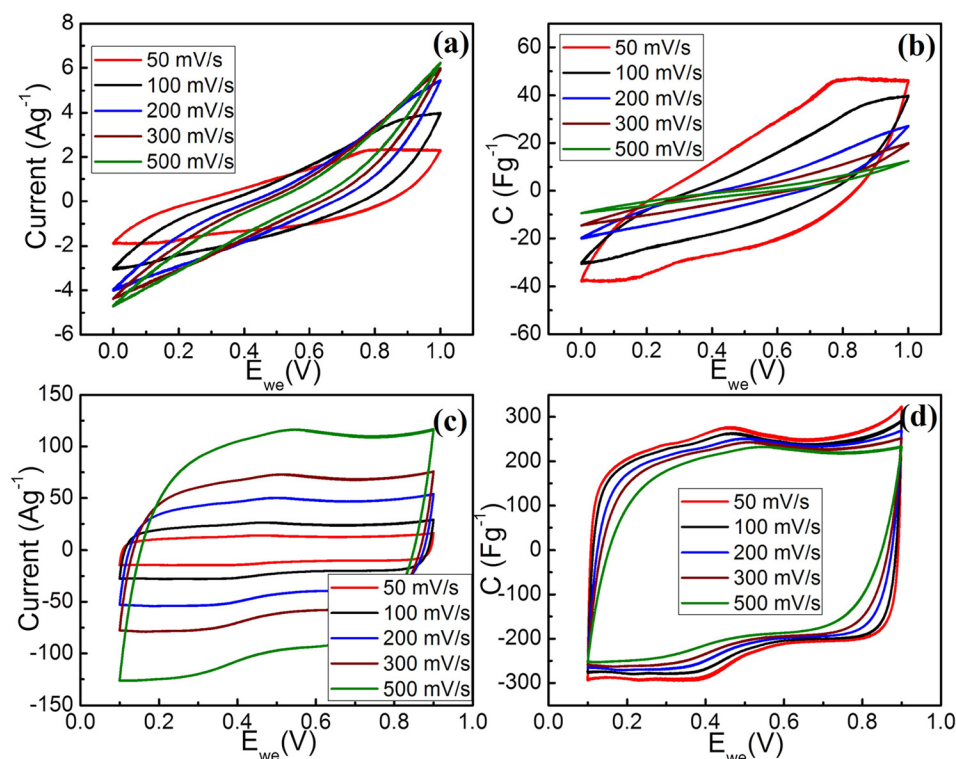


FIG. 3. CV measurements. (a) and (b): Pristine DWCNTs, (c) and (d): U-DWCNTs.

series resistance and insufficient mobility of the ions to reach the pristine DWCNTs electrode at higher scan rates. The electrochemical response of U-DWCNTs electrodes, on the other hand, shows drastic improvement compared to pristine sample. The CV curves at different scan rates and corresponding calculated specific capacitances of the U-DWCNTs electrodes as a function of voltage are shown in Figs. 3(c) and 3(d), respectively. The observed bumps in CV curve may be attributed to the presence of Fe impurities. Groups attached to the dangling bonds such as hydroxyl and carboxyl groups may also cause the irregular shape in the CV curves.<sup>7</sup> The average value of the capacitances calculated over the cycle for scan rates 5, 50, 100, 200, 300, 500  $\text{mV s}^{-1}$  were found to be 270, 240, 226, 211, 198, 178  $\text{Fg}^{-1}$ , respectively. Figs. 3(c) and 3(d) indicate that U-DWCNTs electrode maintains excellent EDLC properties even at very high scan rates which leads to 10–222 times improvements in its specific capacitance compared to the pristine DWCNTs. In Fig. 3(c), the shapes of the CV curves are almost rectangular up to 100  $\text{mV s}^{-1}$ , indicating very good ion accessibility to the surface and low internal series resistance.

Fig. 4(a) shows the specific capacitances of both samples (calculated by integration over the cycle) for different scan rates. The nature of specific capacitance decay with respect to scan rates in pristine DWCNTs sample is exponential while ultrasonicated samples do not follow any exact trend but seems to be linear with two different slopes. This may be attributed to the presence of inhomogeneous pore size distribution in ultrasonicated DWCNTs electrodes that arises from the opened-tip (diameter of tubes is about 2 nm), defects (few nm), and the layered porous structure (few hundreds of nanometer). Therefore, the initial sharp decrease in capacitance in U-DWCNTs (at low scan rates) could be attributed to the narrow pores becoming inaccessible to electrolyte. The much

slower drop in the specific capacitance at high scan rates could arise due to the presence of homogenous and relatively larger size of topographical porous and layered structure in the electrodes. Basically, the as-produced DWCNTs sample consists of densely packed ropes composed of large bundles

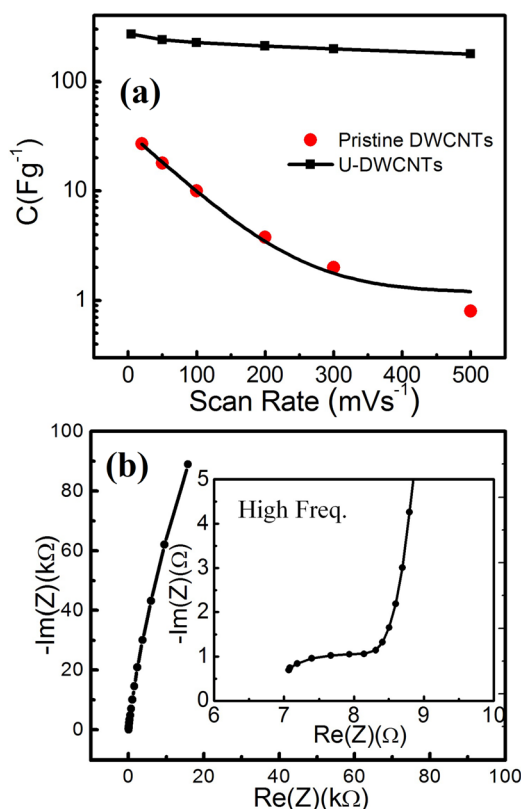


FIG. 4. (a) Specific capacitance versus scan rate of pristine and U-DWCNTs and (b) Nyquist plot of U-DWCNTs in frequency range of 50 kHz–10 mHz (inset: Nyquist plot at high frequency range).



of tubes as shown in Figs. 1(a) and 1(b). Due to the Van der Waals interactions along their sidewalls, it is very hard to access electrolytes to these areas. Due to the transfer of local shear stress during the ultrasonication process in a solution phase of DWCNTs, separation of individual nanotubes from the aggregates or bundles of DWCNTs is achieved. This shear stress imparting on the surface of a DWCNT provides a tensile force, i.e., a pulling effect along the nanotube. Therefore, a continuous high energy ultrasonication for longer duration leads to fractures and/or splitting of CNTs.<sup>14,15</sup> In addition to reduced wall interaction among the tubes, the intense ultrasonication process creates additional defects mostly in form of edges due to the fractures and secessions. Consequently, the electric double layer formation at the carbon nanotube-electrolyte interface increases drastically because of better wettability of electrodes and accessibility of ions to the surface of the sample.<sup>16–18</sup> Additionally, the secessions process opens the closed tips of the U-DWCNTs (Figs. 1(c) and 1(d)) which further enhances the double layer formation at lower scan rates.

In order to investigate the frequency response of the U-DWCNT electrode, electrochemical impedance measurements in 1 M H<sub>2</sub>SO<sub>4</sub> were carried out in the 50 kHz–10 mHz frequency range. An excellent capacitive behavior is evident from the Nyquist plot shown in Fig. 4(b). As expected from our CV measurements, a nearly vertical line has been observed, indicating a pristine EDLC behavior. It shows a linear behavior in low and medium frequency regions, and a deviated arc in high frequency region. In our layered-porous electrode, as the frequency decreases, the deeper and narrower parts of the electrode become accessible to the alternating current, and subsequently more of the electrode surface is available for double layer formation. Furthermore, the impedance behavior in high frequency range (inset of Fig. 4(b)) significantly deviates from the arc, which may be attributed to the presence of a variety of structures such as pores, edges, defects, and curved surfaces, as each shape has different response in this frequency range.<sup>2,7</sup> Considering that the measurements were carried out simply by three-electrode method, the value of interfacial resistance between surface and electrolyte ( $\sim 2 \Omega$ ) is very small. The value of series resistance loss can be reduced down to few mV by providing better conductivity between current

collector and electrodes in properly designed and engineered supercapacitors.

In conclusion, EDLC performance of the DWCNT electrode prepared via intense ultrasonication process has been demonstrated. Ultrasonication, while fracturing and fragmenting DWCNT bundles, introduced opened-tip, edges and defects on the walls of DWCNTs. After ultrasonication U-DWCNT paste formed an excellent layered-porous morphology. These factors contributed to a remarkable enhancement in the EDLC performance of U-DWCNTs electrodes due to increased wettability of electrodes and easier electrolyte ion accessibility.

This research was supported by the WCU (World Class University) program (R31-2008-10029) through the National Research Foundation of Korea (NRF) funded by the Ministry of Education, Science and Technology.

- <sup>1</sup>G. Wang, L. Zhang, and J. Zhang, *Chem. Soc. Rev.* **41**, 797 (2012).
- <sup>2</sup>B. E. Conway, in *Electrochemical Supercapacitors: Scientific Fundamentals and Technological Applications* (Kluwer Academic/Plenum Publishers, New York, 1999).
- <sup>3</sup>E. Frackowiak, K. Metenier, V. Bertagna, and F. Beguin, *Appl. Phys. Lett.* **77**, 2421 (2000).
- <sup>4</sup>R. Kotz, S. Muller, M. Bartschi, B. Schnyder, P. Dietrich, F. N. Buchi, A. Tsukada, G. G. Scherer, P. Rodatz, O. Garcia, P. Barrade, V. Hermann, and R. Gallay, *Proc. - Electrochem. Soc.* **21**, 564 (2001).
- <sup>5</sup>S. Kandalkar, D. Dhawale, C. Kim, and C. Lokhande, *Synth. Met.* **160**, 1299 (2010).
- <sup>6</sup>A. Burke, *Electrochim. Acta* **53**, 1083 (2007).
- <sup>7</sup>R. Kotz and M. Carlen, *Electrochim. Acta* **45**, 2483 (2000).
- <sup>8</sup>P. Simon and Y. Gogotsi, *Nat. Mater.* **7**, 845 (2008).
- <sup>9</sup>H. Pan, J. Li, and Y. P. Feng, *Nanoscale Res. Lett.* **5**, 654 (2010).
- <sup>10</sup>C. Shen, A. H. Brozena, and Y. H. Wang, *Nanoscale* **3**, 503 (2011).
- <sup>11</sup>M. Hoefer and P. R. Bandaru, *Appl. Phys. Lett.* **95**, 183108 (2009).
- <sup>12</sup>P. Rai, S. Pandey, M. Menemparabath, Y. S. Kim, I. H. Lee, P. Nikolaev, and S. Arepalli, *J. Appl. Phys.* **109**, 044308 (2011).
- <sup>13</sup>M. S. Dresselhaus, A. Jorio, A. G. Souza Filho, and R. Saito, *Philos. Trans. R. Soc. London, Ser. A* **368**, 5355 (2010).
- <sup>14</sup>Y. Y. Huang and E. M. Terentjev, *Polymers* **4**, 275 (2012).
- <sup>15</sup>P. Vichchulada, M. A. Cauble, E. A. Abdi, E. I. Obi, Q. Zhang, and M. D. Lay, *J. Phys. Chem. C* **114**, 12490 (2010).
- <sup>16</sup>R. R. Moore, C. E. Banks, and R. G. Compton, *Anal. Chem.* **76**, 2677 (2004).
- <sup>17</sup>C. E. Banks, T. J. Davies, G. G. Wildgoose, and R. G. Compton, *Chem. Commun.* **2005**, 829.
- <sup>18</sup>N. S. Lawrence, R. P. Deo, and J. Wang, *Electroanalysis* **17**, 65 (2005).